Journal of Biomedical Optics

SPIEDigitalLibrary.org/jbo

Rhodamine 800 as a near-infrared fluorescent deposition flow tracer in rodent hearts

Garret Munch
Scott McKay
Eugene Gussakovsky
Bozena Kuzio
Valery V. Kupriyanov
Olga Jilkina

SPIE

Rhodamine 800 as a near-infrared fluorescent deposition flow tracer in rodent hearts

Garret Munch,[a] Scott McKay,[a,b] Eugene Gussakovsky,[c] Bozena Kuzio,[c] Valery V. Kupriyanov,[c,d] and Olga Jilkina[c,e]
[a]University of Manitoba, Department of Chemistry, Winnipeg, Manitoba, R3T 2N2, Canada
[b]University of Manitoba, Department of Physics, Winnipeg, Manitoba, R3T 2N2, Canada
[c]National Research Council of Canada, Institute for Biodiagnostics, 435 Ellice Avenue, Winnipeg, Manitoba, R3B 1Y6, Canada
[d]University of Manitoba, Department of Biochemistry and Medical Genetics, 435 Ellice Avenue, Winnipeg, Manitoba, R3B 1Y6, Canada
[e]University of Manitoba, Department of Oral Biology, 435 Ellice Avenue, Winnipeg, Manitoba, R3B 1Y6, Canada

Abstract. We investigated the use of a near-infrared (NIR) fluorescent dye, Rhodamine 800 (Rhod800, λ_{exc} = 693 nm, λ_{em} > 720 nm) as a flow-dependent molecular tracer for NIR spectroscopy and high-resolution cardiac imaging. Rhod800 accumulates in isolated mitochondria in proportion to the mitochondrial membrane potential ($\Delta\Psi$). However, in the intact myocardium, Rhod800 binding is $\Delta\Psi$-independent. Rat hearts were perfused in a Langendorff mode with Krebs–Henseleit buffer containing 45-nM Rhod800 at normal (100%), increased (150%), or reduced (50%) baseline coronary flow (CF) per gram, for 30 to 60 min. In a different group of hearts, the left anterior descending artery (LAD) was occluded prior to Rhod800 infusion to create a flow deficit area. Rhod800 deposition was analyzed by: 1. absorbance spectroscopy kinetics in the Rhod800-perfused hearts, 2. Rhod800 absorbance and fluorescence imaging in the short-axis heart slices, and 3. dynamic epicardial/subepicardial fluorescence imaging of Rhod800 in KCl-arrested hearts, with a spatial resolution of ~200 μm. Rhod800 deposition was proportional to the perfusate volume (CF and perfusion time) and there was no Rhod800 loss during the washout period. In the LAD-ligated hearts, Rhod800 fluorescence was missing from the no-flow, LAD-dependent endocardial and epicardial/subepicardial area. We concluded that Rhod800 can be used as a deposition flow tracer for dynamic cardiac imaging. [DOI: 10.1117/1.3583581]

Keywords: fluorescence imaging; biomedical optics; spectroscopy; fluorescence; image acquisition/recording; near-infrared.

Paper 11030R received Jan. 17, 2011; revised manuscript received Mar. 31, 2011; accepted for publication Apr. 7, 2011; published online Jun. 1, 2011.

1 Introduction

Assessment of myocardial microperfusion flow is important in the characterization of cardiac disease, where damage to the microvessels (arterioles and capillaries) has been demonstrated or suspected. Most existing myocardial perfusion imaging modalities rely on the distribution of flow tracers that can be divided into two categories: deposition and first-pass. A deposition flow tracer (e.g., microspheres) is retained by the tissue; it can be later detected in the tissue and quantitated.[1,2] Measurements of blood flow using deposition flow tracers are based on the assumption that myocardial tracer content is directly proportional to the flow (per gram of tissue), which would be true if there were complete tracer retention by the tissue.[3] In contrast, a first-pass flow tracer (e.g., indocyanine green) transiently passes through the organ (e.g., heart) and tracer distribution and/or clearance kinetics is determined during this time and used to evaluate the perfusion.[4–6]

Assessment of the blood flow distribution using the microspheres is considered to be the "gold standard."[3] The method relies on deposition of radioactive or colored/fluorescent microspheres (generally, 15 μm in diameter), which are trapped in precapillary arterioles in proportion to the flow per gram of tissue.[1,2] To determine myocardial blood flow distribution, at the end of the experiment the heart is cut into small pieces (no smaller than 0.2 g) and the number of the microspheres is determined by radioactive counting or spectrophotometrically in the tissue lysates. At least 400 microspheres per sample are needed for 5% to 10% statistical accuracy with rather crude spatial resolution (~3 × 3 mm^2 in plane).[7] Rodent models are important tools to study acquired and congenital heart disease. However, conventional microspheres perform poorly in rat hearts (due to their small size of 1 to 1.5 g) and are unreliable in mouse hearts that are approximately 10% of the rat ones by weight.[3,8,9] Optical imaging of fluorescent microspheres permitted a high spatial resolution of up to 37 μm per pixel.[2,10] However, at high resolution (<2 μl or 0.27 mm in one dimension), a nonrandom distribution of the microspheres was demonstrated that was not governed solely by the microflow and chance, but determined by the arteriolar tree branching.[11] There is also a concern that microspheres affect cardiac vascular resistance.[12] The so-called "molecular microspheres" were developed to avoid the embolization problems. These are usually large, lipophilic, radioisotope-labeled molecules such as α–adrenergic agonist, desmethylimipramine (DMI),[13] and an inhibitor of the mitochondrial electron transport chain rotenone.[14] H^3 and $^{125/131}$IDMI digital radiography of rat hearts allowed 6.4 × 6.4 mm^2 region to be resolved in 16×16 pixel or ~400 μm per pixel.[15] To achieve a high spatial

Address all correspondence to: Olga Jilkina, National Research Council of Canada, Institute for Biodiagnostics, 435 Ellice Avenue, Winnipeg, Manitoba, R3B 1Y6, Canada. Tel: 1-204-984-6558; Fax: 1-204-984-7036, E-mail: olga.jilkina@nrc-cnrc.gc.ca.

1083-3668/2011/16(6)/065001/11/$25.00 © 2011 SPIE

resolution and avoid the radiation hazard, it is desirable to investigate other perfusion imaging techniques using flow-dependent nonradioactive molecular tracers.

We have previously studied interaction of a fluorescent dye, Rhodamine 800, (Rhod800, also known as MitoFluor Far Red 680) with the isolated mitochondria, cells, and rat hearts by diffuse reflectance spectroscopy.[16] Rhod800 is a cationic lipophilic dye, whose accumulation in the isolated mitochondria, and, to a lesser extent, cultured cells, is dependent on the mitochondrial membrane potential, $\Delta\Psi$.[16,17] However, in the perfused hearts, retention of Rhod800 as well as that of another closely related dye, tetramethylrhodamine methyl ester, is $\Delta\Psi$-independent, probably due to their excessive hydrophobicity.[16,18] Rhod800 is a near-infrared (NIR) dye: in ethanol, its absorption and fluorescent maxima are at 680 nm and >700 nm, respectively (Molecular Probes technical information). In myocardial tissue, its absorption and fluorescent emission peaks are redshifted to 693 and 720 to 730 nm, respectively.[16] The advantages of using the NIR spectral range for myocardium probing include: deeper tissue penetration (up to several mm)[19] and elimination of interference with the endogenous fluorescent chromophores, such as NAD(P)H and flavoproteins, and quenchers, such as cytochromes; thus, resulting in lower background fluorescence and a better signal-to-noise ratio.[4]

The present study was undertaken to investigate 1. whether Rhod800 fulfills the principle requirements for a deposition flow tracer (i.e., flow-dependent accumulation and tissue retention) and 2. whether this dye can be used for NIR fluorescent perfusion imaging in rodent hearts, in real time.

2 Materials and Methods

The investigation conforms with the "Guide to the Care and Use of Experimental Animals" published by the Canadian Council on Animal Care (Ottawa, Ontario, 1993).

2.1 *Isolation and Perfusion of Rat Hearts*

Male and female Wistar-Kyoto rats (220 to 350 g) were anesthetized with pentobarbital solution. The hearts were removed quickly, and perfused in a Langendorff mode with Krebs–Henseleit buffer (KHB) [in mM, 25 $NaHCO_3$, 118 NaCl, 4.7 KCl, 1.75 $CaCl_2$, 1.2 $MgSO_4$, 0.5 ethylenediamine tetraacetic acid, and 11 glucose, aerated with 95% O_2 and 5% CO_2 to provide PO_2 of ~400 mm Hg].[20] High-potassium KHB (used for live heart imaging) had the same composition as regular KHB, except that 20 mM KCl was added to increase the concentration of K^+ and induce cardiac arrest.[20] To provide the visual contact for optical spectroscopy and imaging all the hearts were perfused in the nonsubmerged state. The temperature of the perfusate was maintained at 36 °C by placing the perfusion tubing inside the temperature-controlled water jacket. The hearts were not paced. Following the placement of a left ventricle (LV) apical drain, a latex balloon was inserted through the mitral valve into the left ventricular cavity and filled with H_2O. The balloon was connected to a pressure transducer and to a Digi-Med Model-210 heart performance analyzer (Micro-Med, Louisville, Kentucky) to monitor the heart rate (HR), LV systolic pressure (LVSP), LV end-diastolic pressure (LVEDP), and perfusion pressure (PP). The coronary flow (CF) was monitored using an ultrasonic blood flow meter (Transonic Systems Inc. Ithaca, New York), and the PP was measured continuously through the catheter connecting the aortic line and the 2nd pressure transducer.

2.1.1 *Perfusion at different CF*

The hearts were perfused for 10 to 15 min under constant PP of approximately 70 mm Hg (set by the height of the buffer reservoir) to establish individual baseline CF rates, which may vary depending mostly on the heart weight. Perfusion was changed to a constant CF mode: a pump was used to control the heart CF rate. The hearts were then randomly divided into three groups: 1. CF remained at 100% (control), 2. increased to 150%, or 3. decreased to 50% of the heart's individual baseline CF rate that was measured in the beginning of the experiment (Table 1).

2.1.2 *LAD-ligation*

To create a perfusion deficit area in selected rat hearts perfused at normal CF, left anterior descending (LAD) artery was ligated using a silk surgical suture 4–0 (Johnson & Johnson, Medical Products, Markham, Ontario, L3R 0T5). As a result, the buffer flow to the part of the LV normally supplied by the LAD stopped and the nonperfused LV area below the ligation point became ischemic. The remote area (e.g., right ventricle, RV) remained adequately perfused and oxygenated.

2.2 *Loading of Rhodamine 800 into Rat Hearts*

Rhodamine 800 (Molecular Probes, Eugene, Oregon) was dissolved in (dimethyl sulfoxide) (Sigma St. Louis, Missouri) to 8 mm, aliquoted and stored at –20 °C until further use when it was diluted in H_2O to a working concentration of 2.7 μm and loaded into a 30-ml syringe. The syringe was placed in a syringe pump set with the infusion flow rate proportional (one-sixtieth) to the CF rate of the heart. Thus, the dye was mixed with KHB at a concentration of 45 nm (Rhod800-KHB) upon entering the hearts.

Rhod800 was loaded in this manner for either 30 or 60 min, after which a 10 min period without the dye was allowed to observe any washout effects. Rhod800 loading was constantly monitored using optical point spectroscopy (see Sec. 2.3 and 2.4) or fluorescence imaging (Sec. 2.5). Long loading times allowed us to study the kinetics of Rhod800 deposition in greater detail. Once the allotted time for introduction of Rhod800 passed, the hearts were removed from the perfusion cannulae and sliced into four short-axis pieces. The slices were then taken for both diffuse reflectance and fluorescence imaging of intramural dye distribution (Sec. 2.6), followed by Rhod800 recovery from the tissue using ethanol extraction (Sec. 2.7).

2.3 *Visible-NIR Point Spectroscopy of Langendorff-Perfused Hearts*

Myocardial absorbance readings were acquired using the technique described elsewhere.[20,21] Briefly, spectra were acquired using an integration time of 0.1 s, an averaging factor of 120 (12-s per acquisition), and a delay of 48 s, thus resulting in a spectrum per minute. Spectra were acquired in the range of 400 to 1100 nm, with a 1-nm increment. Broadband visible/NIR light from a fiber optic illuminator Oriel model 77501 (Stratford,

Table 1 Hemodynamic parameters of Rhod800-KHB-perfused rat hearts.[a]

Group, *n*	CF(ml/min/g)	PP(mm Hg)	HR(beats/min)	LVSP(mm Hg)	LVEDP(mm Hg)
1. Normal/control CF, $n = 13$					
Beginning of perfusion	17.9 ± 3.1	70.2 ± 4.6	206. 5 ± 45.4	117.1 ± 24.5	8.2 ± 6.0
End of perfusion	constant	79.7 ± 12.0	196.7 ± 44.5	140.3 ± 22.7	13.7 ± 5.5
2. Increased CF, $n = 6$					
Beginning of perfusion	27.1 ± 5.0***[b]	132.4 ± 22.5***	186.9 ± 58.4, NS	141.2 ± 12.0*	14.3 ± 6.0, NS
End of perfusion	constant	115.2 ± 21.0	186.7 ± 66.6	141.2 ± 10.5	43.0 ± 23.1$^{\#}$[c]
3. Decreased CF, $n = 10$					
Beginning of perfusion	9.0 ± 1.4***	41. 3 ± 6.7***	168.2 ± 46.5, NS	91.2 ± 12.6**	3.1 ± 5.5*
End of perfusion	constant	40.8 ± 9.6	164.5 ± 54.6	99.9 ± 17.9	0.1 ± 4.7

[a]CF, coronary flow; PP, perfusion pressure; HR, heart rate; LVSP, left ventricular systolic pressure; and LVEDP, left ventricular diastolic pressure. Data are presented as means ± STDEV.
[b]*, **, and ***denotes significant at $p < 0.05$, $p < 0.01$, and $p < 0.001$, respectively; NS, nonsignificant versus control.
[c]# denotes significant at $p < 0.05$ vs. data in the same group in the beginning of perfusion.

Connecticut) was transmitted to the heart through one arm of a bifurcated fiber optic bundle. The common illumination/collection probe tip was placed in contact with the LV perpendicular to the tissue plane with zero distance between them. This configuration allowed the collection of predominantly diffusely reflected light through the second arm of the fiber bundle connected to the spectrometer (model PDA-512, Control Developments Inc., South Bend, Indiana).

Myocardial absorbance (or pseudo-optical density, POD) for any given wavelength was calculated according to the formula:

$$\mathrm{POD} = -\log(I_s/I_0) \quad (1)$$

where I_s is the intensity of the light diffusely reflected by the sample in the back direction and I_0 is the intensity of the light reflected by Spectralon® as a standard.

In the visible-NIR region, the light absorption by hemoglobin-free Rhod800-containing cardiac tissue is mainly determined by myoglobin and Rhod800. The POD spectra of a Rhod800-KHB-perfused rat heart contained the bands of oxygenated myoglobin, with two peaks at 545 and 581 nm, and of Rhod800, with maxima at 635 and 693 nm (Fig. 1). The POD spectrum of the nonperfused part of the myocardium showed the POD bands at 553 and 760 nm, specific for deoxygenated myoglobin (Fig. 2).

2.4 *Kinetics of Rhod800 Absorption Peak at 690 nm in Intact Rat Hearts*

Changes in POD at 690 nm were used to quantify the kinetics of the dye loading in the normal heart. The myocardial POD spectra were processed using GRAMS 32 spectroscopy software (Thermo Scientific, Waltham, Massachusetts). A three-dimensional(3D) multifile was created for each heart by associating all collected 60-s POD spectra (POD versus wavelength, nanometer) with the time points (min) when these spectra were acquired. To correct for the baseline variations, POD at 730 nm was offset to zero. For any chosen heart, time-dependency of Rhod800 absorption at 690 nm was plotted from the multifile data by applying the function "rotate 90 deg" for the 690 nm wavelength.

2.5 *Diffuse Reflectance and Fluorescence Imaging of Rhod800 in the Short-Axes Myocardial Slices*

Both NIR light diffuse reflectance and fluorescence images were captured from the base- and apex-oriented sides of each slice. To perform the diffuse reflectance spectroscopic imaging, the slices were illuminated with an Oriel model 77501 fiber optic illuminator (Stratford, Connecticut) using a 10 mm (core) fiber optics, the output light from which was collimated with a lens.[22] The spectroscopic images were detected with a NIR system consisting of a Hamamatsu C7042 back-thinned FFT-charge coupled device (CCD) camera (Japan), Nikon AF-60 microlens and a Cambridge Research and Instrumentation, Inc. (Woburn, Massachusetts) VariSpec SNIR/NNIR liquid crystal tunable filter (LCTF). The system was assembled and operating software was developed at the NRC Institute for Biodiagnostics. The camera allowed imaging with a resolution of 532 ×256 pixels and frame readout time of 536.8 ms in the 200 to 1100 nm wavelength range. The LCTF worked as an electronically activated tunable interference filter in the range of 650 to 1100 nm with bandwidth of 10 nm and response time of 150 ms. The diffuse reflectance spectrum at each pixel was converted to POD according to Eq. (1). A white polyurethane sponge was employed as a reference. The resulting spectral image was a 3D matrix $Ixy(\lambda)$ [two-dimensional(2D) xy-image of light intensity taken at n wavelengths λ]. A 2D matrix at 690 nm was extracted from the 3D matrix. This wavelength corresponded to the maximum of the far-red absorbance band of Rhod800.

Rhod800 fluorescence images were acquired as described elsewhere.[10,23] Briefly, fluorescence was excited at the red

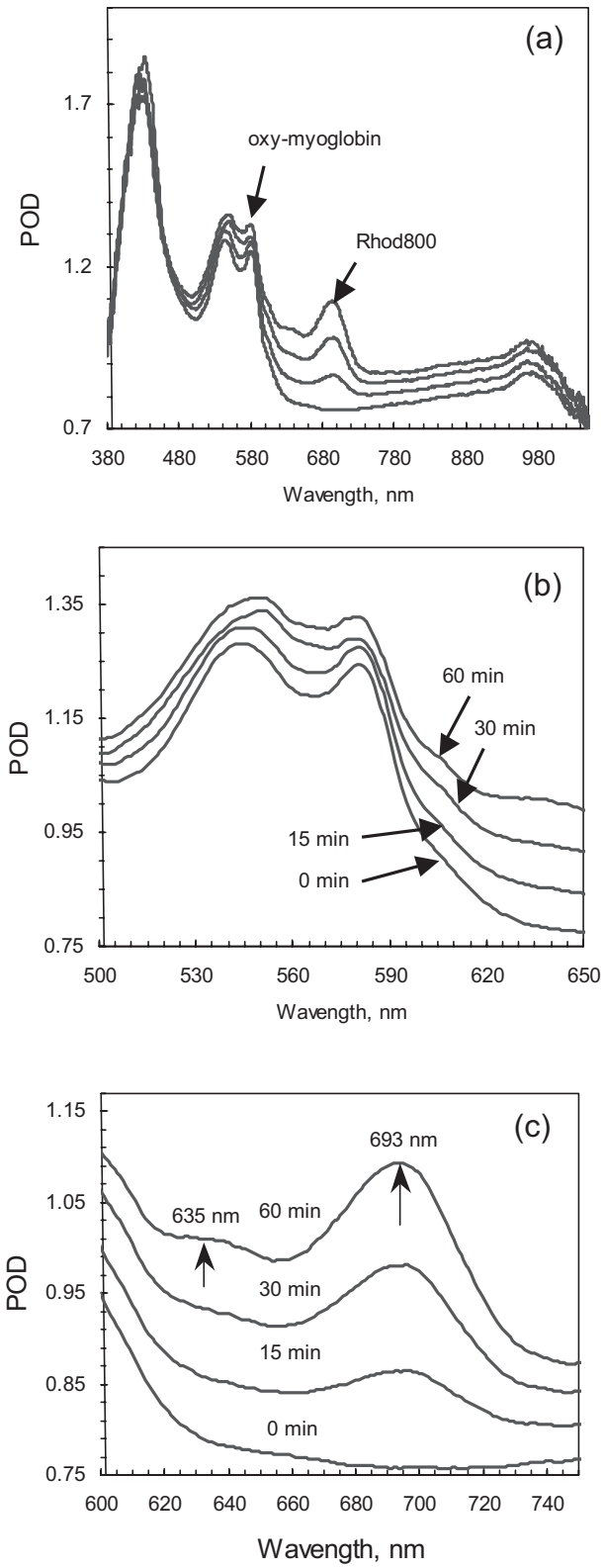

Fig. 1 (a) Myocardial POD spectra of a normal rat heart perfused with KHB and 45-nM Rhod800. Cardiac spectra were taken prior to, 15, 30, and 60 min after Rhod800 infusion started. (b) and (c) Enlarged visible and NIR parts of the spectra. Position of Rhod800 peaks at 635 and 693 nm are indicated with arrows. See Sec. 2 for details.

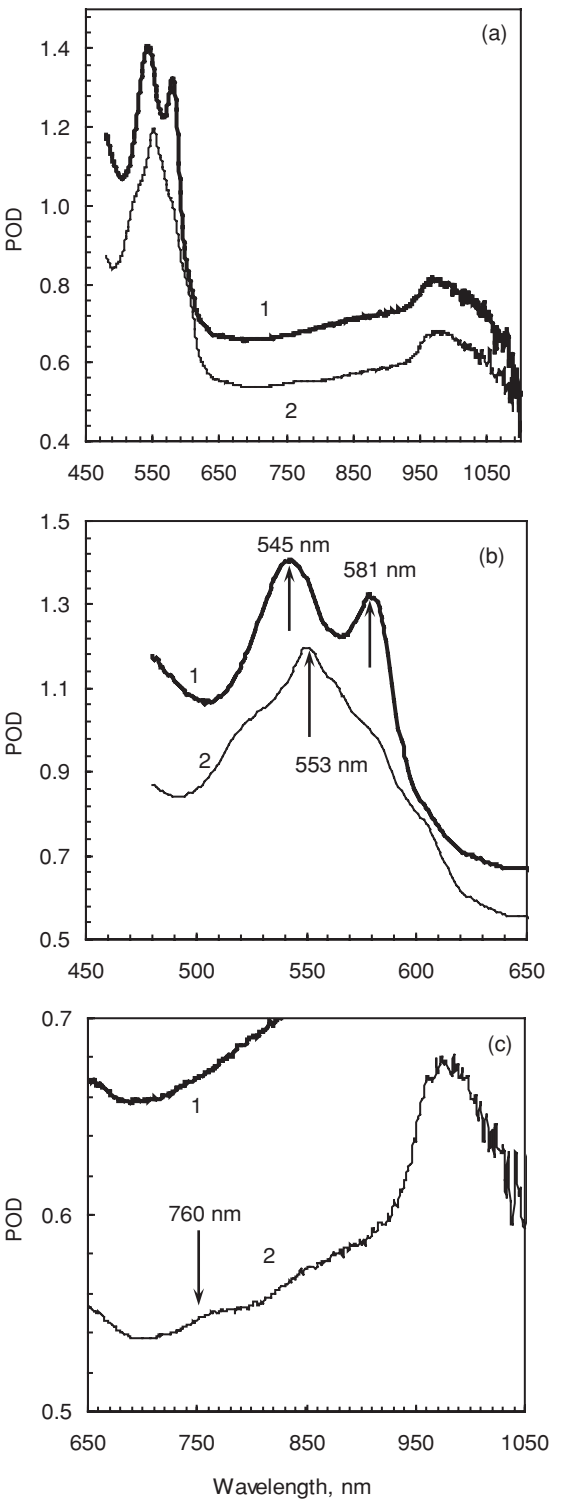

Fig. 2 POD spectra of a representative rat heart with LAD-ligation. No-flow ischemic area was located below LAD ligation point. The spectra were acquired by the fiber optics probe attached to the area of normal (1) or ischemic myocardial tissue (2). (a), (b), and (c) show the same spectra in the wavelength regions of 450 to 1100, 450 to 650 and 650 to 1050 nm, respectively. Position of oxy- (545 and 581 nm) and deoxy- (553 and 760 nm) myoglobin peaks are indicated with arrows.

absorption band of the Rhod800 dye by the light of six laser diodes of 5 mW each (Thorlabs, Newton, New Jersey) emitted a 635-nm noncollimated elliptical light beam. A minimal heterogeneity of such illumination over the surface was corrected for. Fluorescence imaging was performed with a setup, consisted of an infrared-sensitive CCD camera (RS Roper Scientific NTE/CCD-512-EBTF.GR-1, Tucson, Arizona), a Nikon Micro AF60 lens at f/8 and a Schott RG 695 glass filter, which cuts off the excitation light (transmittance of 0.2% at 635 nm). The camera contained a 512×512 back-illuminated CCD element and 14/16-bit ST-138 analog to digital converter run in 14-bit mode (Princeton Instruments, Trenton, New Jersey). A 2×2 binning increased a signal-to-noise ratio and reduced the image size to 256×256 pixels.

The images were processed using MATLAB (The MathWorks, Natick, Massachusetts) programs developed specifically for the current tasks.

2.6 *Time-Resolved Fluorescence Imaging of Live Rhod800-KHB-Perfused Hearts*

The kinetics of the Rhod800 loading into the perfused rat hearts was visualized in 2D by acquiring the fluorescence images of the hearts. To eliminate the artifacts associated with the heart movements, the hearts were arrested by perfusion with the high-potassium KHB prior to Rhod800 infusion. Cardioplegia stopped the heartbeats, but preserved the heart energetics and perfusion. The fluorescence imaging was performed with a PixeLINK CCD USB 2.0 PL-B953 monochrome camera of 1024 × 768 pixel resolution allowing a 2×2 binning to reduce the image size to 512 × 384 pixels. The camera was fitted with a Sigma 24 mm F1.8 EX DG aspherical lens and a Schott RG 695 glass filter. The fluorescence was excited by the 635-nm light of four laser diodes of 5 mW. Each diode emitted a noncollimated elliptical light beam with divergence of about $\pm 5^\circ$ for the short axis and $\pm 15^\circ$ for the long axis of an ellipse at half of maximum intensity. The laser diodes were positioned at about 5 to 7 cm from the heart surface and provided a homogeneous illumination. The images were captured every 60 s. All images were processed using a MATLAB program.

2.7 *Recovery of Rhod800 from Myocardial Tissue*

Once images of the short-axes slices were captured, the slices were cut into smaller pieces that were placed in 1 ml of 95% ethanol in glass vials. The vials were wrapped in tinfoil and left overnight to extract the dye from the tissues. The ethanol preparations were centrifuged and the supernatant was used for the absorbance measurements. Rhod800 concentration was determined using a BioTek Instruments, Inc. microplate reader (Winooski, Vermont) at 680 nm [$\varepsilon = 95\ \mathrm{mM}^{-1}\mathrm{cm}^{-1}$ (Ref. 24)].

If the concentration of Rhod800 in a sample was too low to be detected by its absorbance (<100 nM), it was determined by the fluorescence measurements using SPEX FluoroMax spectrofluorometer (Jobin Yvon Inc., Edison, New Jersey) with a LPS-220 lamp power supply from Photon Technology International (Birmingham, New Jersey) and the SPEX DM 300 software. The concentration was determined from the linear portion of the standard curve generated by using serial dilutions of the known Rhod800 concentrations. The lower Rhod800 concentration detection limit for the fluorescence measurements was 6 nM. Repeated extraction with 95% ethanol recovered ~30% more dye from the myocardial tissue; therefore, the correction factor of 1.3 was used for the single-step ethanol extraction data.

2.8 *Statistics*

Analysis of variance (single factor) was used for data comparison. Differences were considered significant when $P \leq 0.05$. Data are presented as means ± standard deviations unless indicated otherwise.

3 Results

3.1 *Rhod800 Deposition in Hearts Monitored by Diffuse Reflectance Spectroscopy*

3.1.1 *Normal hearts*

Rat hearts were perfused with Rhod800-KHB at normal/control (100%), increased (150%) or decreased (50%) CF (Table 1). Figure 3 shows the kinetics of the Rhod800 dye accumulation in the hearts perfused at different flows. Although a sigmoid shape of the kinetics was evident, the linear fit appeared to be within the standard error; therefore, the saturation state was not reached. Table 2 shows the parameters of the linear regression analysis. The correlation parameter of $R \cong 1$ indicates a high goodness of the fit. The slope of the linear fit reported on the rate of the Rhod800 deposition kinetics. The y-intercept was within the range of ±0.005, which is close to zero with accuracy of 0.5 to 1%. The kinetics rate ratio was closely proportional to the perfusion rate ratio per gram of tissue. No Rhod800 was detected in the cardiac effluent by either absorbance or fluorescence measurements.

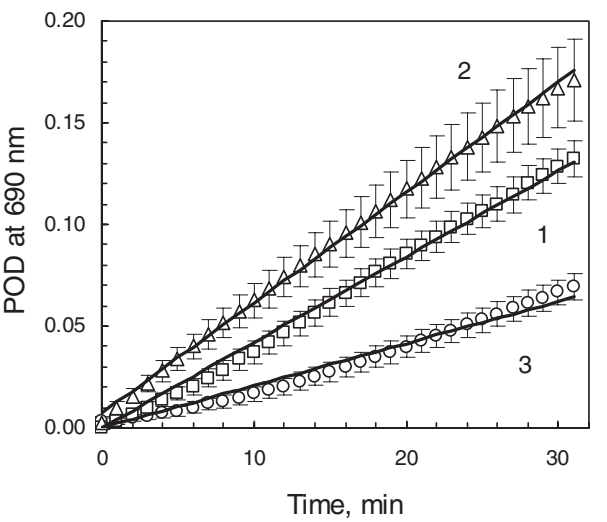

Fig. 3 Dependence of Rhod800 accumulation on the flow in Langendorff-perfused rat hearts. The hearts were randomly perfused with Rhod800-KHB at 100, 150, or 50% of their individual baseline flow. Myocardial POD spectra were taken every 60 s. The average kinetics for 690-nm myocardial POD peak for the hearts perfused at normal (1, open squares), increased (2, open triangles) or decreased (3, open circles) CF are shown (see Sec. 2 for details). Means ± standard error are presented.

Table 2 Kinetics parameters of Rhod800 deposition in beating Rhod800-KHB-perfused rat hearts.[a]

Group, *n*	Perfusion rate ratio,%	Deposition rate $\times 10^3$, min $^{-1}$	*y*-intercept $\times 10^3$	R^2	Deposition rate ratio, %
1. Normal/control CF, $n = 13$	100	4.1	−4.26	0.999	100
2. Increased CF, $n = 6$	151	6.0	7.18	0.999	146
3. Decreased CF, $n = 10$	50	1.9	−3.07	0.992	46
4. Heart with regional flow deficit due to LAD-ligation[b]					
Curve 2 on Fig. 4: normal myocardium	N/A	4.96	−70.2	0.999	N/A
Curve 1a on Fig. 4: non-perfused myocardium; beginning of Rhod800 loading	N/A	0.01	−0.14 ± 7.21	0.625	N/A
Curve 1b on Fig. 4: non-perfused myocardium; end of Rhod800 loading	N/A	−0.03	1.70 ± 1.09	0.891	N/A

[a]To obtain the kinetics parameters of Rhod800 deposition, changes in the amplitude of 690-nm POD peak, specific for Rhod800, were analyzed. For groups 1, 2, and 3, see Fig. 3. The deposition rates were calculated as the slopes of the respective linear regression trend lines. The ratios for the increased and decreased perfusion rates were taken with respect to normal CF per gram of myocardial tissue (see Table 1).
[b]The same rat heart as in Fig. 4 was analyzed.

3.1.2 *Hearts with regional flow deficit*

To demonstrate that POD measurements can be used to identify local perfusion deficits, myocardial spectra were acquired in the Rhod800-perfused LAD-ligated hearts. The fiber optics probe was first placed in contact with the area of the LV wall below LAD ligation, where perfusion was blocked. The border of the no-flow zone was determined by the appearance of hypoxic changes in the myocardial POD spectra (Fig. 2). Once the no-flow area was localized, continuous spectra acquisition from this area was initiated and Rhod800 infusion into the hearts started. The no-flow zone was monitored for ~25 min (Fig. 4). Then, the probe was moved for ~30 min to the RV wall, which was well perfused, and, finally, moved back to the LAD-dependent area to finalize the POD measurements (Fig. 4). Although the perfusate contained Rhod800, no increase of the POD at the dye-specific wavelength (690 nm) was observed in the initial and final stages of the measurements, indicating that no dye deposition took place in the LAD bed of the LV and there was no dye redistribution between the perfused and nonperfused areas. In contrast, the dye deposition was obvious in the RV wall. Table 2 shows that the kinetic parameters for the RV wall with normal myocardium were similar to the deposition rate for the normal heart within 10% error. For the LAD bed, lack of the dye deposition resulted in zero mean value (*y*-intercept) within limits of the standard deviation.

3.2 *Imaging of Rhod800 Absorbance and Fluorescence in the Heart Slices*

Intramural distribution of Rhod800 was evaluated in the short-axes cardiac slices (Table 3, Fig. 5). Absorbance (POD) and fluorescence images demonstrated Rhod800 deposition in the LV and RV walls in normal hearts and lack of deposition in the no-flow zone of the LAD-ligated hearts. Spatial resolution of less than 200 μm was achieved: the heart slice of ~7 mm in diameter was resolved in ~40 pixel. The dark contour around the slice POD images was caused by a nonspecific optical edge effect and should not be taken into consideration.

3.3 *Rhod800 Imaging in Live Hearts*

We investigated whether imaging of Rhod800 fluorescence in the epicardium/subepicardium in intact hearts can be used to visualize perfusion patterns and local perfusion deficits in real-time; thus surface fluorescence images of Rhod800-KHB perfused normal and LAD-ligated hearts were acquired (Fig. 6). No significant autofluorescence was detected in the spectral range used (above 700 nm) prior to the dye loading;

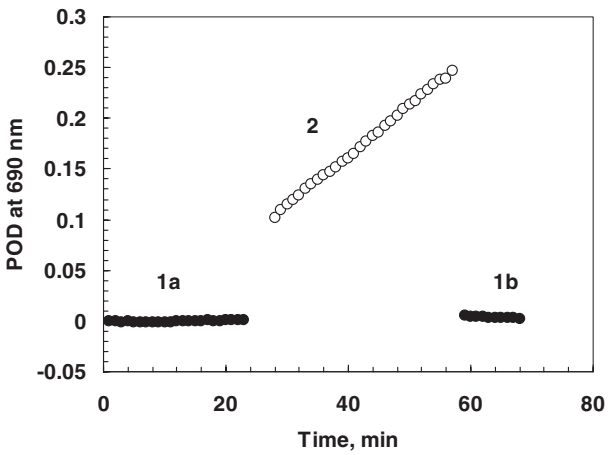

Fig. 4 Kinetics of Rhod800 accumulation a representative Rhod800-KHB-perfused rat heart with LAD-ligation. POD kinetics at 690 nm, the Rhod800-specific maximum, acquired from the no-flow LAD bed (1, filled circles) and normal area (2, open circles) of the same heart are shown. See Sec. 2 for perfusion, LAD-ligation, and spectra acquisition detail.

Table 3 Mean values of POD and fluorescence intensity in normal and ischemic areas of representative rat hearts.[a]

	Normal heart			Heart with LAD ligation		
Myocardium	Normal (LV)	Normal (RV)	LV/RV	Ischemic (LV)	Normal (RV)	LV/RV
POD	0.72 ± 0.06	0.80 ± 0.04	0.90 ± 0.14	0.62 ± 0.05	0.83 ± 0.10	0.75 ± 0.17
n	2197	2016		761	1360	
Fluorescence	0.79 ± 0.09	0.73 ± 0.08	1.08 ± 0.27	0.07 ± 0.02	0.28 ± 0.05	0.24 ± 0.15
n	7763	8077		7039	5506	

[a] *n*, number of pixels in the averaging area of the heart surface in Fig. 5. Fluorescence intensity is in arbitrary units. Pseudo-optical density (POD) of diffuse reflectance at 694 ± 5 nm includes both actual light absorption by chromophores and light scattering inside the cardiac tissue.

therefore, the fluorescence that was registered by the camera was almost exclusively due to the presence of Rhod800 in the epicardial/subepicardial layers of the hearts. Rhod800 fluorescence started to appear when the dye concentration was reaching ~0.3 nmol/g. The images were captured every 60 s for 60 min, with a spatial resolution of ~200 μm. The images demonstrated the presence of Rhod800 fluorescence in the LV and RV walls in normal hearts ($n = 3$) [Fig. 6(a)].

To compare the fluorescence patterns in perfused and non-perfused areas of rat myocardium, surface images of the LAD-ligated, Rhod800-KHB-perfused hearts ($n = 3$) were acquired. These images clearly demonstrated the presence of different fluorescent zones in the myocardium, with varying levels of Rhod800 deposited. Figure 6(b) shows an image of a representative LAD-ligated heart with four regions of interest (ROI) chosen. The least intensive region corresponded to the

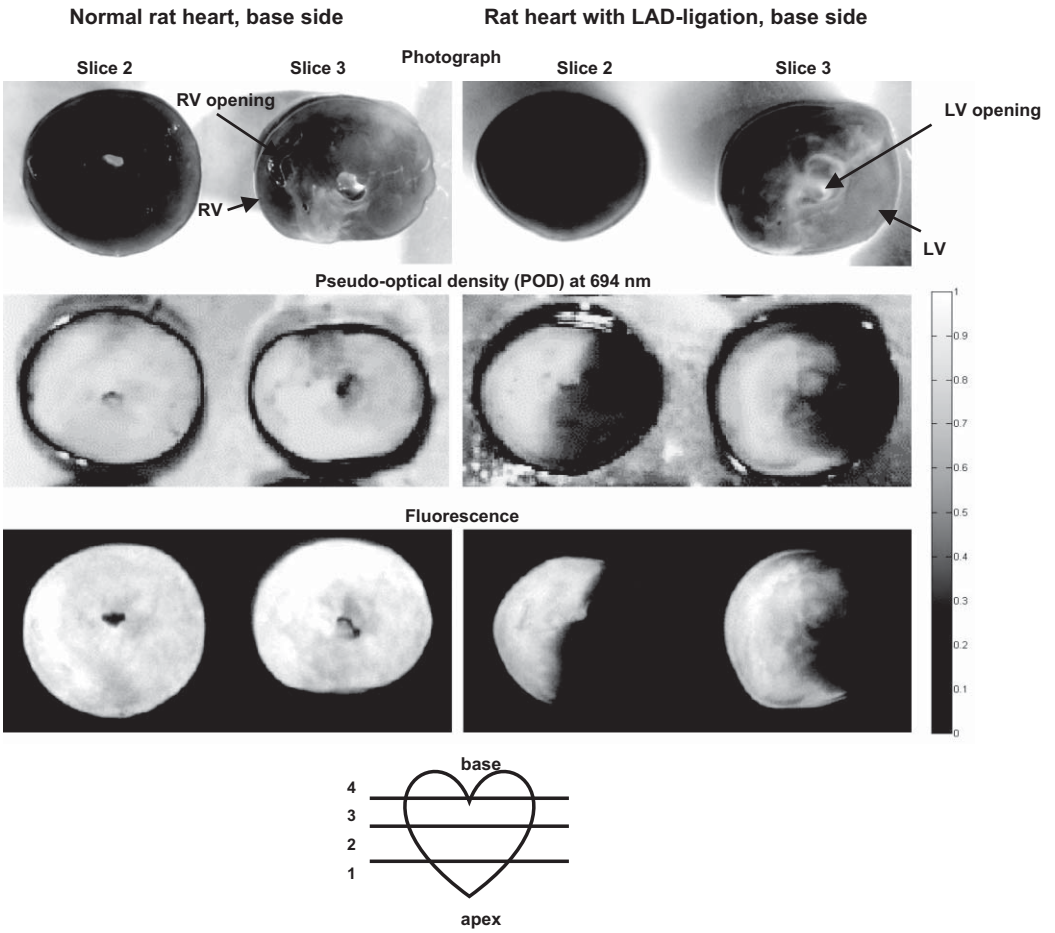

Fig. 5 Rhod800 imaging of the short-axes slices of a normal rat heart and a rat heart with regional perfusion deficit due to LAD ligation. The diagram of the short-axis slices is shown at the bottom. The same slices were first photographed (top panel), then the diffuse reflectance NIR imaging (middle panel) and fluorescence imaging (bottom panel) of these slices were performed as described in Sec. 2. The positions of the LV and RV were as shown on the photograph, for all the slices.

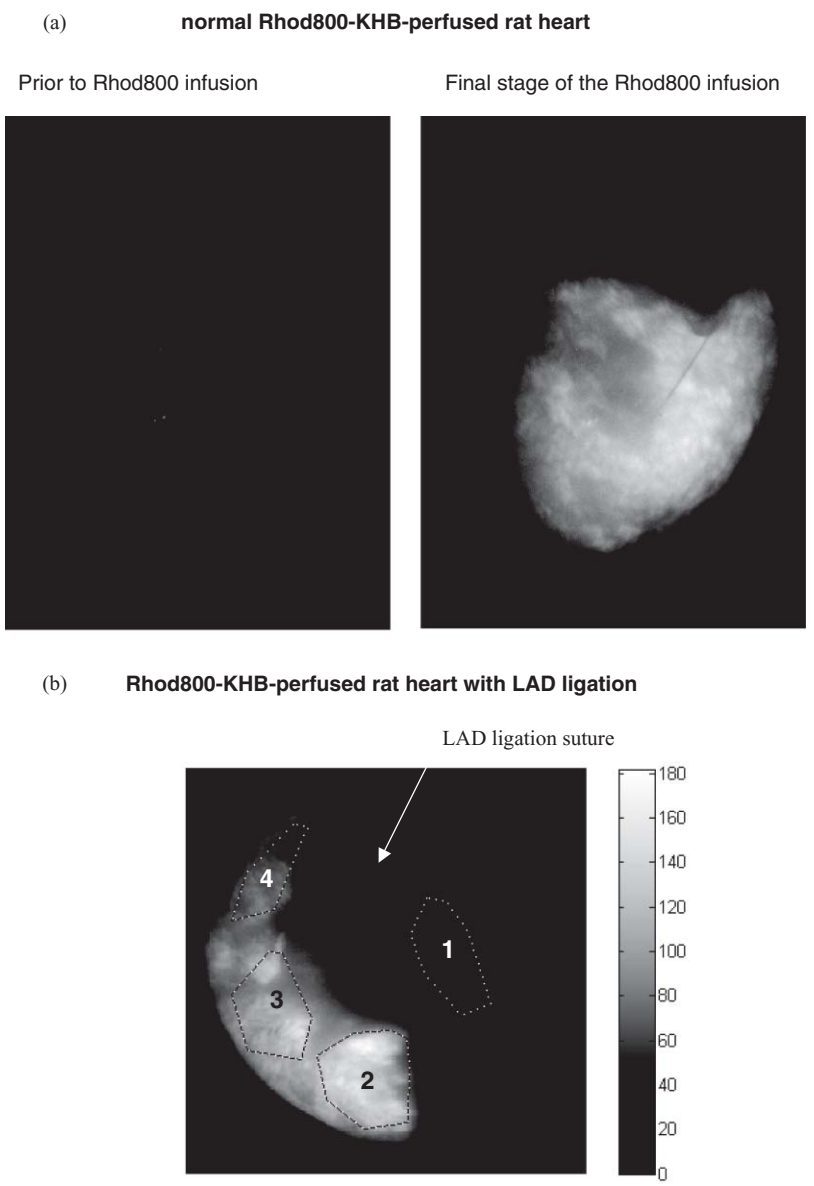

Fig. 6 Fluorescence imaging of live normal and ischemic rat hearts. To eliminate artifacts related to the heart movement, the hearts were perfused with KHB + Rhod800 + KCl, which resulted in cardiac arrest. Two representative rat hearts are shown after 60 min of perfusion: (a) normal and (b) ischemic rat heart, in which LAD was ligated prior to Rhod800 infusion. The hearts were positioned in such a way that both LV and RV were visible and LAD was located on the left side of the view. Black suture that was used for the LAD ligation is indicated with the white arrow on the top left side of the heart in (b). Dotted lines show four ROIs; kinetics of the dye deposition for these areas are shown in Fig. 7. The ischemic area (ROI 1) was located below the suture. Scale is in arbitrary units. See Sec. 2 for details.

LAD bed (ROI 1). Three different ROIs were chosen in the RV, from the base to the apex of the heart. Kinetics of the mean fluorescence intensity over each of the four ROIs are presented in Fig. 7. The arrow indicates a time point when Rhod800 infusion was stopped; however the buffer perfusion continued. There was no change in the Rhod800 fluorescence intensity or patterns during the washout period, thus confirming that the dye deposition was stable and there was no Rhod800 loss from the myocardium. The ratio of intensities for ROI 1 to ROI 3 and 4 (maximal deposition in the RV) taken for the washout period was 0.16 to 0.20. This value was close to the respective value in Table 3 (0.24 ± 0.15) obtained from the slice imaging.

3.4 *Ex-vivo Rhod800 Recovery From Cardiac Tissue*

The relationship between the total amount of Rhod800 delivered to and recovered from each heart with ethanol was investigated. The amount of the dye delivered was calculated as the product of CF, time of perfusion, and Rhod800 concentration in the perfusate. The amount of Rhod800 detected in the ethanol extracts was plotted against the amount of Rhod800 delivered. A linear least square fit was used to obtain the slope $= 0.405$, y-intercept $= -0.142$ (nmol), and the correlation coefficient $R^2 = 0.81$ (Fig. 8). The slope that represented an estimate of the apparent Rhod800 recovery factor was significantly lower than the unity, most likely because of Rhod800 loss during ethanol extraction from the tissue and dye loading, due to

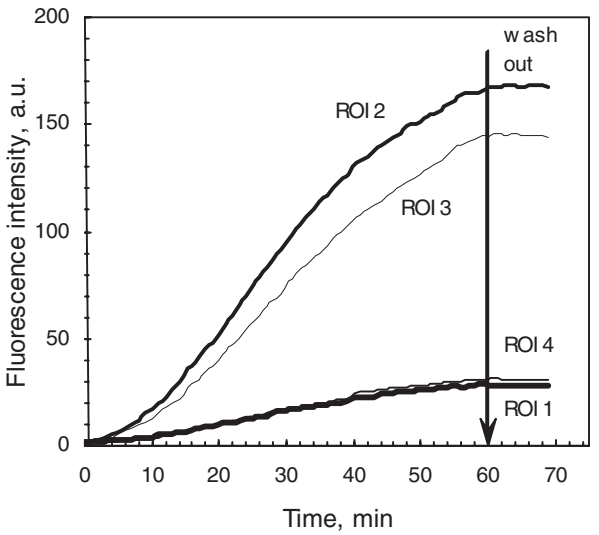

Fig. 7 Kinetics of the Rhod800 dye deposition in LAD-ligated rat heart. To eliminate artifacts related to the heart movement, the hearts were perfused with KHB + Rhod800 + KCl, which resulted in cardiac arrest. Each curve corresponds to the ROI chosen on the fluorescence image as indicated in Fig. 7. The fluorescence intensity in arbitrary units is a mean of intensities in the ROI. After 60 min of the dye loading, the infusion of Rhod800 stopped (indicated by arrow).

partial adsorption of this highly hydrophobic dye on glass and plastic surfaces (e.g., syringe, plastic tubing, etc.). However, a close to zero *y*-intercept and high *R*-value indicated that the correlation took place, and the perfusion flow rate determined the amount of the dye deposited.

3.5 *Cardiac Hemodynamics and Oxygenation*

Perfusion at 50% of the flow resulted in a 40% decrease in PP, and a decrease in LVSP by ~24% (Table 1). In the hearts perfused at 150%, PP increased to ~130 mm Hg (+74%), while the increase in LVSP was only modest by ~21% (Table 1). Changes in HR were not statistically significant. Sixty minute perfusion with Rhod800-KHB at 150% CF resulted in a moderate increase in LVEDP from ~14 to 40 mm Hg (Table 1). The rest of the monitored parameters did not change significantly in any of the groups, following perfusion with Rhod800-KHB.

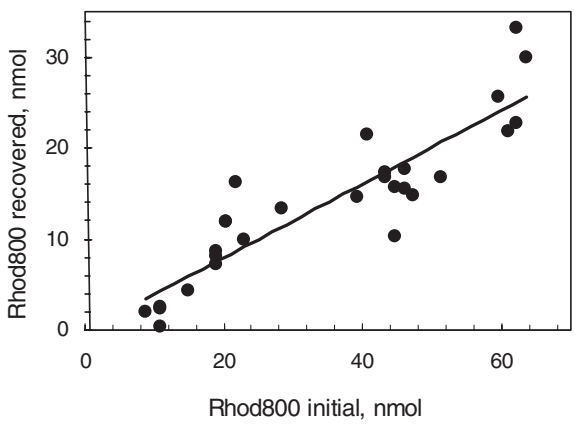

Fig. 8 Linear correlation between Rhod800 loaded into and recovered from Langendorff-perfused rat hearts. The amount of the dye loaded into the hearts was calculated as a product of Rhod800 concentration in the perfusion buffer, CF, and perfusion time. Amount of the dye recovered was determined spectrophotometrically from the ethanol extracts of the heart slices as described in Sec. 2.

Myocardial POD spectra that were acquired provided information not only on the Rhod800 deposition, but also on the oxygenation of the hearts. Myocardial oxygenation is characterized by oxygen saturation parameter (OSP) defined as a ratio of oxygenated to total myoglobin concentration.[25,26] In the present work, OSP was determined using NIR diffuse reflectance measurements in the 700 to 965 nm range as described elsewhere.[21,27] The data for 23 spectra measured from the surface of beating and KCl-arrested rat hearts were averaged: OSP $= 81 \pm 11\%$ for normal and OSP $= 0\%$ for ischemic areas of the hearts. These OSP values are in agreement with the previously published data[21,27] and were not significantly different for beating and KCl-arrested perfused hearts.

The Rhod800 specific 690 nm peak overlaps with the 760-nm deoxy-myoglobin peak in the NIR range [Fig. 2(c)], which makes it impossible to calculate OSP in the hearts containing Rhod800 [Figs. 1(a) and 1(b)]. However, the peaks corresponding to the oxygenated form of myoglobin at 545 and 581 nm were still observed in the visible range [Figs. 1(a) and 1(c)], thus confirming that the dye accumulation, within the concentration range used in this work, did not result in significant hypoxic changes to the hearts.

4 Discussion

4.1 *Dependence of Rhod800 Accumulation on CF in a Langendorff Mode of Perfusion*

Flow-dependence of the Rhod800 deposition in rat hearts was demonstrated by POD spectroscopy measurements in live buffer-perfused rat hearts. During Rhod800-KHB perfusion, myocardial optical density at 690 nm, a wavelength specific to the Rhod800 absorbance, increased linearly over time (Fig. 3). In addition, comparison of the three CF groups demonstrated that rates of the 690-nm peak increase in the live hearts were closely proportional to the CF per gram of tissue (Fig. 3). Since an optical density is a linear function of a chromophore concentration, the *in situ* data imply that Rhod800 concentration in the tissue is linearly proportional to the time of perfusion (i.e., the volume of perfusate passed through the tissue) and CF. This would be expected if all Rhod800 were deposited, which indeed was the case, in the range of concentrations used in this work, as no Rhod800 was detected by either absorbance of fluorescence measurements in the effluent from the Rhod800-perfused hearts. In addition, we have previously demonstrated that Rhod800 deposition in the tissue was very stable: a 30-min washout resulted in only partial dye loss of less than 15%.[16] In comparison, 20% ^{3}HDMI was lost from the myocardium at 3-min post-injection.[15]

A good linear correlation ($R = 0.9$) between the amounts of Rhod800 loaded to the hearts and recovered from the same hearts also confirmed that the dye retention was proportional to the perfusate volume. A deviation of the apparent correlation factor from the unity was likely due to the unavoidable dye loss during recovery of this hydrophobic dye from the tissue as well as during heart loading. In addition, photobleaching that has been demonstrated for other rhodamine derivatives[28]

was possible and could have reduced the apparent dye recovery value. However, since all heart samples were treated equally, the comparative analysis of the dye recovery values was valid.

4.2 *Rhod800 Imaging*

Our previous work has demonstrated the possibility of detecting Rhod800 in tissue using optical point spectroscopy.[16] The novel technical aspect of this work was demonstration of myocardial flow imaging using Rhod800. The major advantage of using Rhod800 is its suitability for real time POD spectroscopy and fluorescence imaging. In fact, acquisition times could be further reduced by eliminating delays between spectra and image acquisition. The conventional microsphere method, although an important technique, is destructive by definition and does not provide the necessary resolution in small hearts.[3] The fluorescent microsphere imaging demonstrated the presence of clusters of the microspheres[2,10] in rat myocardium probably due to their nonrandom distribution and embolization in small (less than 15 μm) arterioles.[11] Rhod800 fluorescence appeared diffuse. Microscopic heterogeneities were observed, however, their analysis was beyond the scope of this work. Use of Rhod800 presents no problems for embolization of the microvessels. While radioactive molecular tracers, such as DMI derivatives,[1,13] are free of the embolization problems, they cannot be used for real-time *in vivo* imaging. Images of the hearts with purposely created local perfusion deficit (short-term infarction caused by LAD ligation) demonstrated that the defects in the myocardial perfusion were easily visualized in both absorbance and fluorescence imaging modes. In the long-term infarction, the scar tissue is usually formed, which is not perfused. It is feasible that Rhod800 could also be used in long-term ischemia similar to another cationic fluorescent dye, IR676, whose absence from the scar tissue in chronically infarcted pig hearts was demonstrated in our lab with the help of diffuse reflectance spectroscopy.[29] IR676 is less studied than Rhod800 and its negative effect on mitochondrial function is more pronounced than that of Rhod800 (Jilkina, unpublished observation). However, some properties, such as high hydrophobicity, are similar between Rhod800 and IR676; therefore, we expect that, similar to IR676, Rhod800 will not be deposited in the myocardial scar tissue.

4.3 *Comparison of Light Absorption and Fluorescence Detection*

Unlike absorbance reading, the fluorescence signal can be used only for semi-quantitative Rhod800 distribution analysis. Indeed, Rhod800 fluorescence intensity increase deviates from linearity upon Rhod800 loading and washout due to fluorescence quenching, formation of nonfluorescent dimers, changes in quantum yield caused by the dye intracellular redistribution and binding to lipid membranes, etc.[16,30,31] However, fluorescence imaging is far more sensitive than absorbance imaging thus allowing better detection of perfusion deficits using a very low dye concentration in the tissue (below 1-μm threshold). To demonstrate which of the methods is the most appropriate, Table 3 presents the ratios of the mean values of POD and fluorescence intensity found for the normal and nonperfused areas of the hearts. In the no-flow zone, POD was reduced by about 25% while fluorescence was reduced by 75%. The reasons for this discrepancy include a significant contribution to POD of internal light scattering, which mimics the real POD determined by the dye light absorption. In contrast, the fluorescence depends almost exclusively on Rhod800 deposited in the myocardium. It is possible, however unlikely (as POD spectroscopy data demonstrated, see Fig. 4) that nonzero fluorescence intensity in the ischemic area resulted from a partial dye penetration from the RV to the LV wall. In addition, a small portion of the excitation light scattered from the heart surface could have contributed to the measured signal because of nonzero transmittance (0.2% at the excitation wavelength) of the cutoff filter.

4.4 *Mitochondrial Binding of Rhod800*

In isolated energized mitochondria ($\Delta\Psi = -160$ mV), Rhod800 is taken up due to its positive charge; it is released by the uncoupled mitochondria.[16,17] However, we have previously demonstrated that in the myocardium, Rhod800 accumulation is $\Delta\Psi$-independent.[16] Upon Rhod800 release from the mitochondria, the dye remains passively bound to the plasma membrane, endo/sarcoplasmic reticulum and polyanions, such as DNA/RNA due to its high hydrophobicity and, therefore, changes in $\Delta\Psi$ do not affect Rhod800 retention in the tissue.[16] Other lipophilic mitochondria-binding deposition tracers, such as rotenone-derivatives, have been used to evaluate myocardial flow in buffer- and erythrocyte-perfused animal hearts;[14] while ^{99m}Tc-Sestamibi, a lipophilic cationic myocardial perfusion tracer that also accumulates in mitochondria, is already in clinical use.[32] However, a different mitochondrial stain, MitoTracker (molecular probes) caused immediate death when injected into animals thus raising the concern for the possible toxic side effects for the mitochondria-binding dyes *in vivo*.[33] Rhod800 can be detected in blood at a concentration as low as 2 μm.[34] Rhod800 is known to inhibit mitochondrial respiration in states 3 and 4 in the isolated mitochondria at the concentrations above 10 μm.[17] We have observed only a slight inhibition of cardiac contractile function[16] and no significant effect on vascular resistance caused by accumulation of up to $\sim$10 μm Rhod800 in the tissue (see normal flow group in Table 1). In the increased flow group, the final Rhod800 concentration reached $\sim$15 μm. This high concentration of Rhod800 could have affected the mitochondrial function, thus resulting in less efficient functioning of the ATP-dependent calcium pump[35] leading to an increase in intracellular calcium and heart's stiffness (Table 1). Alternatively, the increase in coronary perfusion (pressure and flow) also known to modulate intracellular calcium[36] was primarily responsible for the LVEDP increase. Thus, use of Rhod800 *in vivo* might be possible, but deserves a cautious pilot testing.

5 Conclusion

This work demonstrated that: 1. Rhod800 deposition in the myocardial tissue is stable and flow dependent, and 2. high-resolution ($\sim$200 μm) fluorescence imaging of intramural (*ex vivo*) and epicardial/subepicardial perfusion deficits (in real time) is attainable using tissue concentrations of Rhod800 in the low micromolar range, in the NIR spectral region, devoid of the background fluorescence.

Acknowledgments

This research was supported, in part, by an operating grant from the Manitoba Health Research Council to O.J.

References

1. J. B. Bassingthwaighte, M. A. Malone, T. C. Moffett, R. B. King, S. E. Little, J. M. Link, and K. A. Krohn, "Validity of microsphere depositions for regional myocardial flows," *Am. J. Physiol.* **253**, H184–H193 (1987).
2. S. L. Hale, M. T. Vivaldi, and R. A. Kloner, "Fluorescent microspheres: a new tool for visualization of ischemic myocardium in rats," *Am. J. Physiol.* **251**(2), H863–H868 (1986).
3. F. W. Prinzen and J. B. Bassingthwaighte, "Blood flow distributions by microsphere deposition methods," *Cardiovasc. Res.* **45**(1), 13–21 (2000).
4. J. V. Frangioni, "In vivo near-infrared fluorescence imaging," *Curr. Opin. Chem. Biol.* **7**(5), 626–634 (2003).
5. D. P. Taggart, B. Choudhary, K. Anastasiadis, Y. Abu-Omar, L. Balacumaraswami, and D. W. Pigott, "Preliminary experience with a novel intraoperative fluorescence imaging technique to evaluate the patency of bypass grafts in total arterial revascularization," *Ann. Thorac. Surg.* **75**(3), 870–873 (2003).
6. V. V. Kupriyanov, S. Nighswander-Rempel, and B. Xiang, "Mapping regional oxygenation and flow in pig hearts in vivo using near-infrared spectroscopic imaging," *J. Mol. Cell. Cardiol.* **37**(5), 947–957 (2004).
7. G. D. Buckberg, J. C. Luck, D. B. Payne, J. I. Hoffman, J. P. Archie, and D. E. Fixler, "Some sources of error in measuring regional blood flow with radioactive microspheres," *J. Appl. Physiol.* **31**(4), 598–604 (1971).
8. K. H. Hiller, P. Adami, S. Voll, F. Roder, P. Kowallik, W. R. Bauer, A. Haase, and G. Ertl, "In vivo colored microspheres in the isolated rat heart for use in NMR," *J. Mol. Cell. Cardiol.* **28**(3), 571–577 (1996).
9. S. Wetterlin, K. F. Aronsen, I. Björkman, and I. Ahlgren, "Studies on methods for determination of the distribution of cardiac output in the mouse," *Scand. J. Clin. Lab. Invest.* **37**(5), 451–454 (1977).
10. E. Gussakovsky, B. Kuzio, Y. Yang, and V. Kupriyanov, "Fluorescence imaging to quantify the fluorescent microspheres in cardiac tissue," *J. Biophotonics.* [Epub ahead of print] (2010).
11. U. K. Decking, V. M. Pai, E. Bennett, J. L. Taylor, C. D. Fingas, K. Zanger, H. Wen, and R. S. Balaban, "High-resolution imaging reveals a limit in spatial resolution of blood flow measurements by microspheres," *Am J Physiol Heart Circ Physiol.* **287**(3), H1132–H1140 (2004).
12. C. J. Zuurbier, B. Kruyver, O. Eerbeek, E. G. Mik, and C. Ince, "Commonly used numbers of microspheres affect cardiac vascular resistance," *J. Cardiovasc. Pharmacol.* **41**(2), 223–232 (2003).
13. S. E. Little and J. B. Bassingthwaighte, "Plasma-soluble marker for intraorgan regional flows," *Am. J. Physiol.* **245**(4), H707–H712 (1983).
14. R. C. Marshall, P. Powers-Risius, B. W. Reutter, S. E. Taylor, H. F. VanBrocklin, R. H. Huesman, and T. F. Budinger, "Kinetic analysis of ^{125}I-iodorotenone as a deposited myocardial flow tracer: comparison with ^{99m}Tc-sestamibi," *J. Nucl. Med.* **42**(2), 272–281 (2001).
15. T. Matsumoto, T. Asano, M. Takemoto, H. Tachibana, Y. Ogasawara, and F. Kajiya, "Microheterogeneity of regional myocardial blood flows in low-perfused rat hearts evaluated by double-tracer digital radiography," *Appl. Radiat. Isot.* **65**(8), 910–917 (2007).
16. O. Jilkina, H. J. Kong, L. Hwi, B. Kuzio, B. Xiang, D. Manley, M. Jackson, and V. V. Kupriyanov, "Interaction of a mitochondrial membrane potential-sensitive dye, rhodamine 800, with rat mitochondria, cells, and perfused hearts," *J. Biomed. Opt.* **11**(1), 014009 (2006).
17. J. Sakanoue, K. Ichikawa, Y. Nomura, and M. Tamura, "Rhodamine 800 as a probe of energization of cells and tissues in the near-infrared region: a study with isolated rat liver mitochondria and hepatocytes," *J. Biochem.* **121**(1), 29–37 (1997).
18. R. C. Scaduto, Jr. and L. W. Grotyohann, "Measurement of mitochondrial membrane potential using fluorescent rhodamine derivatives," *Biophys. J.* **76**(1), 469–477 (1999).
19. S. P. Nighswander-Rempel, V. V. Kupriyanov, and R. A. Shaw, "Assessment of optical path length in tissue using neodymium and water absorptions for application to near-infrared spectroscopy," *J. Biomed. Opt.* **10**, 024023 (2005).
20. O. Jilkina, B. Kuzio, G. J. Grover, C. D. Folmes, H. J. Kong, and V. V. Kupriyanov, "Sarcolemmal and mitochondrial effects of a K_{ATP} opener, P-1075, in 'polarized' and 'depolarized' Langendorff-perfused rat hearts," *Biochim. Biophys. Acta.* **1618**(1), 39–50 (2003).
21. E. Gussakovsky, O. Jilkina, Y. Yang, and V. Kupriyanov, "Hemoglobin plus myoglobin concentrations and near infrared light pathlength in phantom and pig hearts determined by diffuse reflectance spectroscopy," *Anal. Biochem.* **382**(2), 107–115 (2008).
22. E. Gussakovsky, Y. Yang, J. Rendell, O. Jilkina, and V. V. Kupriyanov, "Mapping the myoglobin concentration, oxygenation, and optical pathlength in heart ex vivo using near-infrared imaging," *Anal Biochem.* **407**, 120–127 (2010).
23. E. Gussakovsky and Y. Yang, "On the emission intensity of fluorescent microsphere in cardiac tissue images," *J. Fluoresc.* **20**, 857–863 (2010).
24. R. P. Haugland, "Probes for organelles," Chap. 12 in *Handbook of Fluorescent Probes and Research Products. Ninth Edition*, J. Gregory and M. T. Z. Spence, Eds., pp. 469–502, Molecular Probes, Inc., Eugene, OR (2002).
25. O. Jilkina, M. Glogowski, B. Kuzio, P. A. Zhilkin, E. Gussakovsky, and V. V. Kupriyanov, "Defects in myoglobin oxygenation in K_{ATP}-deficient mouse hearts under normal and stress conditions characterized by near infrared spectroscopy and imaging," *Int. J. Cardiol.* [Epub ahead of print] (2010).
26. R. A. Shaw, V. V. Kupriyanov, O. Jilkina, and M. G. Sowa, "Near-infrared in vivo spectroscopic imaging: Biomedical research and clinical applications," Chap. 8 in *Raman, IR, and NIR Chemical Imaging*, S. Sasic and Y. Ozaki, eds., pp. 149–165, John Wiley & Sons, New York (2010).
27. E. Gussakovsky, O. Jilkina, Y. Yang, and V. V. Kupriyanov, "Noninvasive measurements of hemoglobin + myoglobin, their oxygenation and NIR light pathlength in heart in vivo by diffuse reflectance spectroscopy," *Proc. SPIE* **7161**, 71612L (2009).
28. N. A. George, B. Aneeshkumar, P. Radhakrishnan, and C. P. G. Vallabhan, "Photoacoustic study on photobleaching of Rhodamine 6G doped in poly(methyl methacrylate)," *J. Phys. D: Appl. Phys.* **32**, 1745–1749 (1999).
29. Y. Yang, J. Sun, P. Gervai, M. L. Gruwel, O. Jilkina, E. Gussakovsky, X. Yang, and V. Kupriyanov, "Characterization of cryoinjury-induced infarction with manganese-and gadolinium-enhanced MRI and optical spectroscopy in pig hearts," *Magn. Reson. Imaging* **28**, 753–766 (2010).
30. R. I. MacDonald, "Characteristics of self-quenching of the fluorescence of lipid-conjugated rhodamine in membranes," *J. Biol. Chem.* **265**, 13533–13539 (1990).
31. K. Sekiguchi, S. Yamaguchi, and T. Tahara, "Formation and dissociation of rhodamine 800 dimers in water: steady-state and ultrafast spectroscopic study," *J. Phys. Chem. A* **110**(8), 2601–2606 (2006).
32. P. A. Carvalho, M. L. Chiu, J. F. Kronauge, M. Kawamura, A. G. Jones, B. L. Holman, and D. Piwnica-Worms, "Subcellular distribution and analysis of technetium-99m-MIBI in isolated perfused rat hearts," *J. Nucl. Med.* **33**(8), 1516–1522 (1992).
33. F. Brasch, M. Neckel, R. Volkmann, G. Schmidt, G. Hellige, and F. Vetterlein, "Mapping of capillary flow, cellular redox state, and resting membrane potential in hypoperfused rat myocardium," *Am. J. Physiol.* **277**(5), H2050–H2064 (1999).
34. O. O. Abugo, R. Nair, and J. R. Lakowicz, "Fluorescence properties of rhodamine 800 in whole blood and plasma," *Anal. Biochem.* **279**(2), 142–150 (2000).
35. H. Pouleur, "Diastolic dysfunction and myocardial energetic," *Eur. Heart J.* **11**, 30–34 (1990).
36. M. Kitakaze and E. Marban, "Cellular mechanism of the modulation of contractile function by coronary perfusion pressure in ferret hearts," *Physiol.* **414**, 455–472 (1989).